Available online at www.sciencedirect.com
ScienceDirect
Journal of Solid State Chemistry 180 (2007) 3152–3159
JOURNAL OF SOLID STATE CHEMISTRY
www.elsevier.com/locate/jssc

# Titanium-based mixed oxides from a series of titanium(IV) citrate complexes

Yuan-Fu Deng[a,b], Hua-Lin Zhang[a], Qi-Ming Hong[a], Wei-Zheng Weng[a], Hui-Lin Wan[a], Zhao-Hui Zhou[a,*]

[a]*Department of Chemistry and State Key Laboratory of Physical Chemistry of Solid Surfaces, Xiamen University, Xiamen 361005, China*
[b]*College of Chemistry Science, South China University of Technology, Guangzhou 510640, China*

Received 12 December 2006; received in revised form 26 April 2007; accepted 31 August 2007
Available online 19 September 2007

**Abstract**

The isostructural hexaaquatransition-metal/titanium citrate complexes $(NH_4)_2[M(H_2O)_6][Ti(H_2cit)_3]_2 \cdot 6H_2O$ [$M$(II) = Mn **1**, Fe **2**, Co **3**, Ni **4**, Cu **5**, and Zn **6**] ($H_4$cit = citric acid), which were synthesized by reacting titanium(IV) citrate with divalent metal salts in the 1.0–3.5 pH range, adopt hydrogen-bonded chain motifs. The crystal structures feature three bidentate citrate anions that chelate to the titanium atom through their negatively charged α-alkoxy and α-carboxy oxygen atoms; the chelation is consistent with the large downfield shifts of $^{13}C$ NMR for carbon atoms for complex **6**. The thermal decomposition of the complexes furnishes mixed metal oxides. The main-group magnesium analog when heated at 600 °C yielded $MgTi_2O_5$ that is of the pseudobrookite type; the particle size is approximately 30 nm.
© 2007 Elsevier Inc. All rights reserved.

*Keywords:* Titanium(IV); Divalent metals; Citrate; Water cluster; Mixed oxides; Crystal structure

## 1. Introduction

As citratotitanate(IV) complexes with counter-cations such as barium and calcium can be readily converted to barium and calcium titanate upon thermal treatment, some studies have been devoted to examining their compositions and structural information through a wide range of physical techniques [1–3]. In our own work, we have found the basic structural unit of the molecular precursor for the titanium citrate, feature three bidentate [$(HO_2CCH_2)_2$–$C(CO_2$–$)O$–] citrato groups that chelate to the titanium atom through their negatively charged α-alkoxyl and α-carboxyl oxygen atoms; while the other two β-carboxylic acid groups are free [4]. Here we continue our studies with the preparations of titanium-based mixed oxides from a series of titanium(IV) citrate complexes $(NH_4)_2[M(H_2O)_6][Ti(H_2cit)_3]_2 \cdot 6H_2O$ [$M$ = Mn (**1**), Fe (**2**), Co (**3**), Ni (**4**), Cu (**5**), Zn (**6**) and Mg (**7**)] with novel dodecameric water clusters. These complexes have been tried to use as molecular precursors for the preparations of mixed oxides with stoichiometry $MTi_2O_5$ ($M$ = Mn, Fe, Co, Ni, Cu, Zn and Mg).

## 2. Experimental section

### 2.1. Preparation of $(NH_4)_2[Mn(H_2O)_6][Ti(H_2cit)_3]_2 \cdot 6H_2O$ (*1*)

Manganese carbonate (0.60 g, 5.0 mmol) was added to an aqueous solution of titanium tetrachloride (1.9 g, 10 mmol, 5 mL) and citric acid monohydrate (6.3 g, 30 mmol). Ammonium hydroxide (1 M) was added to the mixture to a pH of 2.0. The filtered solution yielded colorless crystals in 40% yield. CH&N elemental analysis for $C_{36}H_{34}O_{54}N_2Ti_2Mn$. Found (Calcd): C 27.9 (28.0); H 4.4 (4.4); N 1.7 (1.8). IR (KBr): $\nu_{(COOH)}$ $1712_{vs}$, $\nu_{as(COO)}$ $1597_{vs}$, $\nu_{s(COO)}$ $1445_m$, $1142_m$, $1385_s$, $1305_s$, $\nu_{(Ti-O)}$ $665_m$, $563_s$.

*Corresponding author.
*E-mail address:* zhzhou@xmu.edu.cn (Z.-H. Zhou).

0022-4596/$ - see front matter © 2007 Elsevier Inc. All rights reserved.
doi:10.1016/j.jssc.2007.08.033

### 2.2. Preparation of $(NH_4)_2[Fe(H_2O)_6][Ti(H_2cit)_3]_2 \cdot 6H_2O$ (2)

Iron powder (0.30 g, 5.0 mmol) in place of manganese carbonate afforded the light green crystals of **2** in 80% yield. CH&N elemental analysis for $C_{36}H_{34}O_{54}N_2Ti_2Fe$. Found (Calcd): C 27.9 (28.0); H 4.3 (4.4); N 1.7 (1.8). IR (KBr): $\nu_{(COOH)}$ $1712_{vs}$, $\nu_{as(COO)}$ $1597_{vs}$, $\nu_{s(COO)}$ $1445_m$, $1425_{ms}$, $1385_s$, $1305_s$, $\nu_{(Ti-O)}$ $665_{m,}$ $563_{s.}$ The formulation was confirmed by the comparison of its unit cell constants with those of the published compound [4b].

### 2.3. Preparation of $(NH_4)_2[Co(H_2O)_6][Ti(H_2cit)_3]_2 \cdot 6H_2O$ (3)

Citric acid monohydrate (6.3 g, 30 mmol) was in 10 mL of water was reacted with titanium *n*-buthoxide (3.4 g, 10 mmol). On completion of the reaction, the water was removed and the residue was redissolved in 20 mL of water; $CoCl_2 \cdot 6H_2O$ (1.2 g, 5.0 mmol) was then added followed by ammonium hydroxide (1 M) to a pH of 2.0. Pink crystals were obtained in 60% yield after a week. CH&N elemental analysis for $C_{36}H_{34}O_{54}N_2Ti_2Co$. Found (Calcd): C 28.0 (28.0); H 4.3 (4.4); N 1.7 (1.8). IR (KBr): $\nu_{(COOH)}$ $1712_{vs}$, $\nu_{as(COO)}$ $1597_{vs}$, $\nu_{s(COO)}$ $1445_m$, $1425_m$, $1385_s$, $1303_s$, $\nu_{(Ti-O)}$ $665_{m,}$ $563_{s.}$

### 2.4. Preparation of $(NH_4)_2[Ni(H_2O)_6][Ti(H_2cit)_3]_2 \cdot 6H_2O$ (4)

The use of $NiCl_2 \cdot 6H_2O$ (1.2 g, 5.0 mmol) in place of $CoCl_2 \cdot 6H_2O$ gave light green crystals of **2** in 70% yield. CH&N elemental analysis for $C_{36}H_{34}O_{54}N_2Ti_2Co$. Found (Calcd): C 28.0 (27.9); H 4.3 (4.4); N 1.7 (1.8). IR (KBr): $\nu_{(COOH)}$ $1712_{vs}$, $\nu_{as(COO)}$ $1597_{vs}$, $\nu_{s(COO)}$ $1445_m$, $1425_m$, $1385_s$, $1305_s$, $\nu_{(Ti-O)}$ $665_{m,}$ $563_{s.}$

### 2.5. Preparation of $(NH_4)_2[Cu(H_2O)_6][Ti(H_2cit)_3]_2 \cdot 6H_2O$ (5)

The use of $CuCl_2 \cdot 2H_2O$ (0.85 g, 5.0 mmol) in place of $CoCl_2 \cdot 6H_2O$ gave light blue crystals of **2** in 60% yield. CH&N elemental analysis for $C_{36}H_{34}O_{54}N_2Ti_2Co$. Found (Calcd): C 28.0 (27.9); H 4.3 (4.4); N 1.7 (1.8). IR (KBr): $\nu_{(COOH)}$ $1712_{vs}$, $\nu_{as(COO)}$ $1597_{vs}$, $\nu_{s(COO)}$ $1445_m$, $1425_m$, $1385_s$, $1304_s$, $\nu_{(Ti-O)}$ $665_{m,}$ $563_{s.}$

### 2.6. Preparation of $(NH_4)_2[Zn(H_2O)_6][Ti(H_2cit)_3]_2 \cdot 6H_2O$ (6)

The use of ZnO (0.40 g, 5.0 mmol) in place of manganese carbonate in the first synthesis afforded the colorless crystals of **6** in 80% yield. CH&N elemental analysis for $C_{36}H_{34}O_{54}N_2Ti_2Fe$. Found (Calcd): C 27.9 (27.8); H 4.4 (4.4); N 1.7 (1.8). IR (KBr): $\nu_{(COOH)}$ $1712_{vs}$, $\nu_{as(COO)}$ $1597_{vs}$, $\nu_{s(COO)}$ $1445_m$, $1425_m$, $1385_s$, $1305_s$, $\nu_{(Ti-O)}$ $665_{m,}$ $563_{s.}$ $^1H$ NMR $\delta_H$ (500 MHz, $D_2O$): 2.723 (d, $J = 14.5$ Hz, $CH_2$), 2.956 (d, $J = 14.5$ Hz, $CH_2$); $^{13}C$ NMR $\delta_C$ ($D_2O$): 188.4 $(CO_2)_\alpha$; 176.2 $(CO_2)_\beta$; 90.7 (≡CO); 45.7 ($CH_2$).

### 2.7. Pyrolysis of the precursors

A 1 g sample of the complex (**1**–**7**) was placed in a porcelain dish and calcined at 300 °C for 2 h in air to give an amorphous material that was further calcined for 2 h in air at 600, 700, 800, or 900 °C.

### 2.8. Physical measurements

Infrared spectra were recorded as Nujol mulls between KBr plates with Nicolet 360 FT-IR spectrometer. Elemental analyses were performed on EA 1110 elemental analyzers. $^1H$ NMR and $^{13}C$ NMR spectra were recorded on a Varian UNITY 500 NMR Spectrometer with sodium 2,2-dimethyl-2-silapentane-5-sulfonate as internal reference. Thermal gravimetric (TG) and differential thermal analyses (DSC) were carried out on an SDT Q600 Instrument at a heating rate 10 °C/min in air–$N_2$ atmosphere. Diffractograms were obtained by using a Rigaku D/Max-C powder diffractometer (Cu-*K*α radiation) at 40 KV and 30 mA, at a scan rate of 4°/min. The morphology of the calcined product was measured on an FEI Tecnai F30 transmission electron microscope (TEM).

### 2.9. X-ray structure determination

Single-crystal diffraction measurements were made on a Bruker Smart Apex CCD area-detector diffractometer with graphite monochromate Mo-*K*α radiation ($\lambda = 0.71073$ Å) at 296 K. The data were corrected for absorption effects [5a]. The structures were primary solved by the SHELXS-97 routine in the WinGX package [5b] and refined by full-matrix least-squares procedures with anisotropic thermal parameters for all the non-hydrogen atoms with SHELXL-97 [6]. Summaries of crystallographic data for **1**–**6** are given in Table 1. Selected bond distances and angles of the complexes are listed in Table 2.

## 3. Results and discussions

### 3.1. Syntheses

The syntheses of *M*(II)–titanium(IV) citrate complexes reported here were expediently carried out in aqueous solution at pH = 1.0–3.0. The mol ratio of divalent metal ion, titanium(IV) ion and citric acid seems no to be crucial for the formations of these species. Control of the ratio of divalent metal ion, titanium(IV) ion, and citric acid (1:2:6) in the synthesis will drive the reaction completely and lead to the isolation of titanium(IV) citrate complexes in high yield. The presence of ammonia in the reaction mixture was essential. It aided in the adjustment of the pH of the reaction mixture, and provided the necessary counterion for balancing the charge on the derived anionic complex.

Table 1
Crystal data summaries of intensity data collections and structure refinements for $(NH_4)_2[M(H_2O)_6][Ti(H_2cit)_3]_2 \cdot 6H_2O$ [$M$ = Mn (**1**), Fe (**2**), Co (**3**), Ni (**4**), Cu (**5**), and Zn (**6**)]

| Empirical formula | $C_{36}H_{68}O_{54}N_2Ti_2Mn$ (**1**) | $C_{36}H_{68}O_{54}N_2Ti_2Fe$ (**2**) | $C_{36}H_{68}O_{54}N_2Ti_2Co$ (**3**) | $C_{36}H_{68}O_{54}N_2Ti_2Ni$ (**4**) | $C_{36}H_{68}O_{54}N_2Ti_2Cu$ (**5**) | $C_{36}H_{68}O_{54}N_2Ti_2Zn$ (**6**) |
|---|---|---|---|---|---|---|
| Formula weight | 1543.66 | 1544.57 | 1547.65 | 1547.43 | 1552.26 | 1554.09 |
| Crystal color | Colorless | Light green | Light red | Light green | Light blue | Colorless |
| Crystal system | Hexagonal | | | | | |
| Cell constants | | | | | | |
| $a$ (Å) | 15.642(1) | 15.4413(7) | 15.5441(8) | 15.562(2) | 15.493(1) | *15.5390(9)* |
| $c$ (Å) | 7.7078(5) | 7.6252(3) | 7.5964(7) | 7.690(1) | 7.6802(6) | 7.6954(8) |
| $V$ (Å$^3$) | 1633.2(2) | 1574.52(9) | 1610.3(2) | 1605.5(3) | 1596.5(2) | 1609.2(2) |
| Space group | *P–3* | | | | | |
| Formula units/unit cell | 1 | | | | | |
| $D_{calc}$ (g cm$^{-3}$) | 1.570 | 1.629 | 1.596 | 1.600 | 1.615 | 1.604 |
| $\mu$ (mm$^{-1}$) | 0.551 | 0.601 | 0.620 | 0.657 | 0.698 | 0.735 |
| $F_{000}$ | 799 | 800 | 801 | 802 | 803 | 804 |
| Diffractometer | Smart Apex CCD | | | | | |
| Radiation | Mo $K\alpha$ ($\lambda = 0.7107$ Å) | | | | | |
| Reflections collected/ unique | 12 969/2590 [$R$(int) = 0.0725] | 18 283/2417 [$R$(int) = 0.0929] | 9812/2523 [$R$(int) = 0.0784] | 9724/2432 [$R$(int) = 0.0987] | 11 405/1873 [$R$(int) = 0.0806] | 9841/2514 [$R$(int) = 0.0982] |
| Data/restraints/ parameters | 2590/11/166 | 2417/11/166 | 2523/11/166 | 2432/11/166 | 1873/11/166 | 2514/11/166 |
| $\theta$ range (°) | 1.50–28.19 | 1.52–27.50 | 1.51–28.28 | 1.51–27.48 | 1.52–24.98 | 1.51–28.25 |
| GOF on $F^2$ | 1.011 | 1.053 | 1.073 | 0.743 | 1.107 | 0.963 |
| $R_1$, w$R_2$ [$I > 2\sigma(I)$][a] | 0.050, 0.111 | 0.044, 0.113 | 0.048, 0.109 | 0.062, 0.151 | 0.074, 0.159 | 0.058, 0.099 |
| $R_1$, w$R_2$ (all data) | 0.071, 0.118 | 0.051, 0.117 | 0.064, 0.116 | 0.117, 0.193 | 0.088, 0.168 | 0.100, 0.111 |
| Largest diff. peak and hole (e Å$^{-3}$) | 0.424, −0.479 | 0.477, −0.434 | 0.380, −0.509 | 0.424, −0.479 | 0.748, −0.526 | 0.584, −0.492 |

[a] $R_1 = \Sigma\{||F_o|-|F_c||\}/\Sigma(|F_o|)$, w$R_2 = \Sigma[w(F_o^2-F_c^2)^2]/\Sigma[w(F_o^2)^2]^{1/2}$.

Table 2
Selected bond distances (Å) and angles (°) for $(NH_4)_2[M(H_2O)_6][Ti(H_2cit)_3]_2 \cdot 6H_2O$ [$M$ = Mn (**1**), Fe (**2**), Co (**3**), Ni (**4**), Cu (**5**), and Zn (**6**)]

| | **1** | **2** | **3** | **4** | **5** | **6** |
|---|---|---|---|---|---|---|
| Ti(1)–O(1) | 1.873(2) | 1.855(1) | 1.866(2) | 1.867(3) | 1.868(3) | 1.868(2) |
| Ti(1)–O(2) | 2.056(2) | 2.035(1) | 2.052(2) | 2.052(3) | 2.050(3) | 2.047(2) |
| $M$(1)–O(1w) | 2.164(2) | 2.094(2) | 2.083(2) | 2.051(3) | 2.065(4) | 2.080(3) |
| O(1)–Ti(1)–O(2) | 78.55(6) | 78.62(5) | 78.71(6) | 78.4(1) | 78.4(1) | 78.69(9) |
| O(1)–Ti(1)–O(1a) | 95.78(6) | 95.74(5) | 95.77(6) | 95.9(1) | 95.7(1) | 95.7(1) |
| O(1)–Ti(1)–O(2a) | 107.68(7) | 107.68(7) | 107.63(7) | 107.7(1) | 107.7(1) | 107.83(9) |
| O(1)–Ti(1)–O(2b) | 156.25(7) | 156.28(6) | 156.33(7) | 156.1(1) | 156.1(1) | 156.19(9) |
| O(2)–Ti(1)–O(2b) | 81.24(7) | 81.21(6) | 81.10(7) | 81.4(1) | 81.4(1) | 81.1(1) |
| *Hydrogen bonding* | | | | | | |
| **1** | O4···O3(c) | 2.640(2) | 171(3) | O6···O7(d) | 2.673(2) | 171(3) |
| | O1w···O5(e) | 2.791(3) | 173(3) | O2w···O3(f) | 2.785(2) | 167(3) |
| **2** | O4···O3(c) | 2.610(2) | 169(3) | O6···O7(d) | 2.645(3) | 171(3) |
| | O1w···O5 | 2.755(2) | 177(2) | O2w···O3 | 2.770(2) | 179(2) |
| **3** | O4···O3(c) | 2.632(3) | 174(3) | O6···O7(d) | 2.660(3) | 170(3) |
| | O1w···O5 | 2.791(3) | 176(3) | O2w···O3(e) | 2.788(2) | 166(2) |
| **4** | O4···O3(c) | 2.631(5) | 171(5) | O6···O7(d) | 2.656(5) | 169(5) |
| | O1w···O5(e) | 2.794(5) | 170(5) | O2w···O3 | 2.790(5) | 168(5) |
| **5** | O4···O3(c) | 2.628(5) | 172(6) | O6···O7(d) | 2.658(5) | 167(6) |
| | O1w···O5 | 2.788(6) | 164(6) | O2w···O3(e) | 2.716(6) | 154(5) |
| **6** | O4···O3(c) | 2.632(3) | 178(4) | O6···O7(d) | 2.668(4) | 176(4) |
| | O1w···O5 | 2.793(4) | 163(3) | O2w···O3 | 2.788(3) | 173(3) |

Symmetric transformations:
**1**: a: 1−$y$, $x-y+1$, $z$; b:−$x+y$, 1−$x$, $z$; c: $x$, $y$, $-1+z$; d: 1−$x$, −1−$y$, 1−$z$; e: $x$, $y+1$, $z$; f: $x-y-1$, $x$, 1−$z$.
**2**: a: $-x+y$, −1−$x$, $z$; b: −1−$y$, $x-y-1$, $z$; c: $x$, $y$,−1+$z$; d: 1−$x$, 1−$y$, 2−$z$.
**3**: a:−$x+y$ +1, 1−$x$, $z$; b: 1−$y$, $x-y$ +1, $z$; c: $x$, $y$,−1+$z$; d: 1−$x$,−$y$, 2−$z$; e: $x-y$, $x$, 2−$z$.
**4**: a:−$x+y$,−1−$x$, $z$; b:−1−$y$, $x-y-1$, $z$; c: $x$, $y$,−1+$z$; d: 1−$x$,−1−$y$,−$z$; e: $y$,−$x+y$,−$z$.
**5**: a:−$x+y+1$,−$x$, $z$; b:−$y$, $x-y-1$, $z$; c: $x$, $y$,−1+$z$; d:−$x$, 1−$y$, 2−$z$; e: $x-y$, $x$, 2−$z$.
**6**: a:−$x+y$,−1−$x$, $z$; b:−1−$y$, $x-y-1$, $z$; c: $x$, $y$,−1+$z$; d:−$x$,−1−$y$, 2−$z$.

All the complexes are soluble in aqueous solutions, especially in hot water and slightly soluble in the organic solvent such as ethanol and acetone. These compounds constitute ideal candidates as precursors for the preparations of multimetallic oxides, which involve the well-defined water-soluble transition metal complexes. Moreover, the use of ammonium cations as counterions and citric acid ligand was particularly welcome to avoid residual contamination of the final materials upon thermal degradation.

In an attempt to explore the speciation of the $M$(II)–Ti(IV)–citrate ternary system in aqueous solution when pH $>3.0$, it was found that different divalent metal citrate complexes were isolated in different pH conditions. For examples: when pH 4.0–5.0 was maintained, the solutions containing $M$(II) ion ($M=$ Mn and Co), titanium(IV) ion, and citric acid deposited $(NH_4)_{2n}[M_2(Hcit)_2(H_2O)_2]_n$ [7a]; when Cu(II) or Zn(II) ion exists in the titanium citrate solution at pH = 4.0–5.0, $[Cu_2(cit)]_n \cdot 2nH_2O$ and $[Zn(H_2O)]_{2n}[Zn(Hcit)_2]_n$ were obtained respectively [8,9a]. Moreover, controls of the pH value in the range of 6.0–7.0, the complexes with the molecular formula $(NH_4)_4[M(Hcit)_2] \cdot H_2O$ [$M=$ Mn(II) [10], Co(II) [7b], Cu(II) [8b], Zn(II) [9], $x=0$; $M=$ Ni(II) [11], $x=2$] were isolated as reported previously. These observations are a clear indication that the formations of $M$(II)–titanium(IV) citrate complexes are typically pH-dependent reaction patterns. Citrate ligand shows better coordination ability toward titanium(IV) ion than divalent metal ions at low pH value. However, the citrate ligand is prone to coordinate the divalent metal ions in weak acidic or neutral medium, which is related to the hydrolysis of titanium(IV) ion.

### 3.2. Description of the crystal structures

The seven compounds are all isostructural. As such, only the structure of complex **1** (Fig. 1) need to be described.

The titanium atom is six-coordinate in an octahedral environment through coordination by three α-alkoxy groups and three α-carboxy groups from three citrate ligands. The binding mode is similar to that found in the previously reported titanium(IV) citrate complexes isolated from different pH conditions [4,12–14]. On the other hand, the metal atom of the cation is surrounded by six water molecules in an octahedral arrangement. The free β-carboxylic acid groups interact with the deprotonated α-carboxy groups [2.640(2) Å] and the β-carboxy groups [2.673(3) Å] of an adjacent molecule through hydrogen bonds to result in the formation of the network structure (as shown in Fig. S2). The network motif appears to be the key factor for stabilizing such citrate complexes. The anionic network interacts with the $[M(H_2O)_6]^{2+}$ counterions (Fig. S3).

The crystal structure also features a dodecameric water cluster built around a cyclic chair hexameric core (Fig. 2, Table 3). Other $(H_2O)_{12}$ clusters have been noted in inorganic [15] and metal-organic [16] compounds; however,

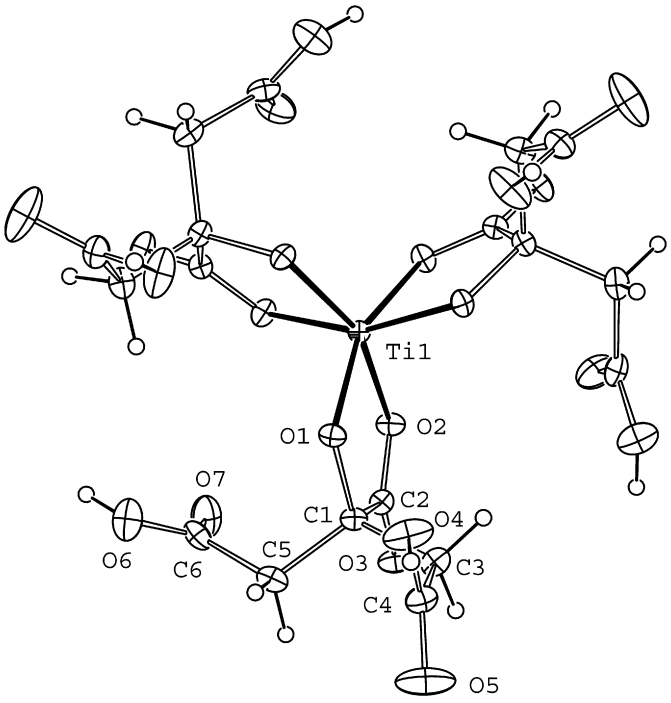


Fig. 1. ORTEP plot of $[Ti(H_2cit)_3]^{2-}$ anion in $(NH_4)_2[Mn(H_2O)_6][Ti(H_2cit)_3]_2 \cdot 6H_2O$ (**1**) in $\Lambda$ configuration at 20% probability level.

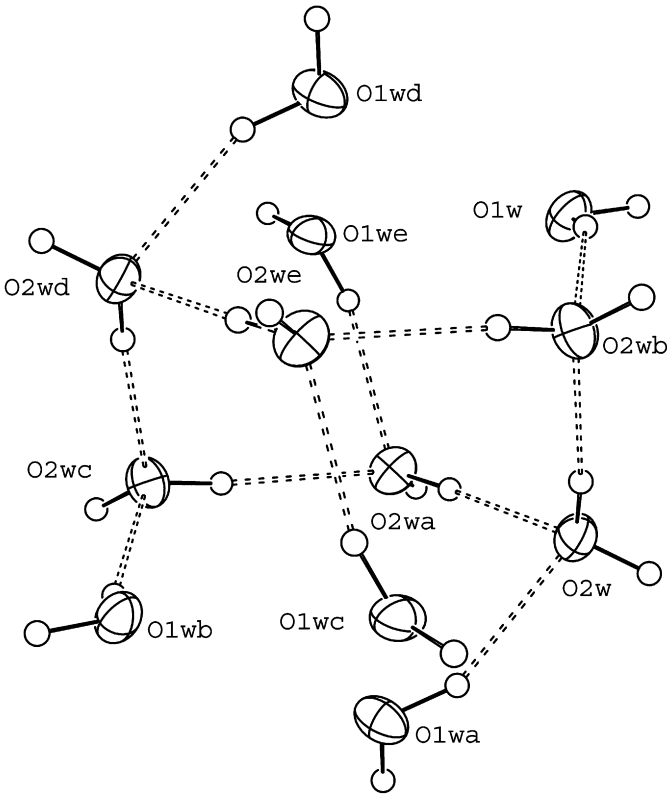


Fig. 2. ORTEP plot of a dodecameric water cluster showing hydrogen-bonding interactions in $(NH_4)_2[Mn(H_2O)_6][Ti(H_2cit)_3]_2 \cdot 6H_2O$ (**1**) at 30% probability level.

the $(H_2O)_{12}$ cluster in the present study represents a new mode of association of water molecules. Among the twelve water molecules, the six water molecules in the center adopt a cyclic chair conformation. In the cyclic hexamer, the average O···O distances is found to be 2.840 Å that compares well with the distance in liquid water [17]. The bulk water exhibits a short range O···O order in the X-ray diffraction radial distribution curve at 2.850 Å, while for the gas phase, this value is ~0.1 Å longer. The O···O distances between the water molecule at the core and the neighbor are 2.728 Å, indicating that the water hexamer is stabilized not only by the formation of hydrogen bonds, but also by the coordination of water molecules. Six of the water molecules in the dodecameric water cluster bind to the metal ions, resulting in an infinite metal–water chain (Fig. 3).

Of the divalent metal–titanium citrate complexes reported, only Ti(IV) cation coordinated to citrate ligand, while the other divalent metal ions coordinated to six water molecules, forming $[M(H_2O)_6]^{2+}$ cations. Simultaneously, these hexahydrated cations form metal–water chains. Carefully examined the metal ions' radius [$Mn^{2+}$ 0.83, $Fe^{2+}$ 0.78, $Co^{2+}$ 0.75, $Ni^{2+}$ 0.69, $Cu^{2+}$ 0.73, $Zn^{2+}$ 0.83, and $Mg^{2+}$ 0.72 Å] and the bond distances of the hydrated complexes [$Mn^{2+}$–$O_w$ 2.164(2), $Fe^{2+}$–$O_w$ 2.094(2), $Co^{2+}$–$O_w$ 2.083(2), $Ni^{2+}$–$O_w$ 2.051(2), $Cu^{2+}$–$O_w$ 2.065, $Zn^{2+}$–$O_w$ 2.080, and $Mg^{2+}$–$O_w$ 2.053(2) [4a] Å] in the metal–water chains, it is found the formations of metal–water chains are not related to the size of divalent ions between 0.69 and 0.83 Å [18]. That is, the metal–water chain is the basic feature of the super-structure, which is important for the construction of this series of divalent metal–titanium citrate complexes.

Comparisons of the Ti–$O_{\alpha\text{-alkoxy}}$ and Ti–$O_{\alpha\text{-carboxy}}$ distances for titanium(IV) citrate complexes show that they are very similar. The average Ti–$O_{\alpha\text{-alkoxy}}$ bond

Table 3
Geometrical parameters of hydrogen bonds for the water cluster for $(NH_4)_2[M(H_2O)_6][Ti(H_2cit)_3]_2 \cdot 6H_2O$ [$M$ = Mn (**1**), Fe (**2**), Co (**3**), Ni (**4**), Cu (**5**), Zn (**6**), and Mg (**7**)]

| | D–H···A | D–H | H ···A | D ···A | D–H ···A | Symmetry |
|---|---|---|---|---|---|---|
| (**1**) | O1w–H1w1···O2w | | 1.95 | 2.728(3) | 153(3) | $x, y, z$ |
| | O2w–H2w2···O2w | | 1.99 | 2.804(2) | 173(3) | $x-y, x, 1-z$ |
| (**2**) | O1w–H1w1···O2w | | 1.90 | 2.710(2) | 158(3) | $y, -x+y, 2-z$ |
| | O2w–H2w2···O2w | | 1.95 | 2.795(2) | 175(3) | $y, -x+y, 2-z$ |
| (**3**) | O1w–H1w1···O2w | | 1.94 | 2.731(3) | 155(3) | $x, y, z$ |
| | O2w–H2w2···O2w | 0.85 | 1.97 | 2.812(3) | 170(2) | $x-y, x, 2-z$ |
| (**4**) | O1w–H1w1···O2w | | 1.90 | 2.733(4) | 150(5) | $x, y, z$ |
| | O2w–H2w2···O2w | | 1.96 | 2.807(4) | 176(4) | $x-y, x, -z$ |
| (**5**) | O1w–H1w1···O2w | | 1.93 | 2.716(5) | 154(5) | $x, y, z$ |
| | O2w–H2w2···O2w | | 1.96 | 2.803(5) | 174(4) | $x-y, x, 2-z$ |
| (**6**) | O1w–H1w1···O2w | | 1.91 | 2.731(4) | 163(4) | $y, -x+y, 2-z$ |
| | O2w–H2w2···O2w | | 1.97 | 2.809(3) | 173(3) | $y, -x+y, 2-z$ |
| (**7**) | O1w–H1w1···O2w | | 1.89 | 2.736(3) | 170(3) | $y, -x+y, -z$ |
| | O2w–H2w2···O2w | | 1.97 | 2.803(3) | 164(3) | $-y, x, 1-z$ |

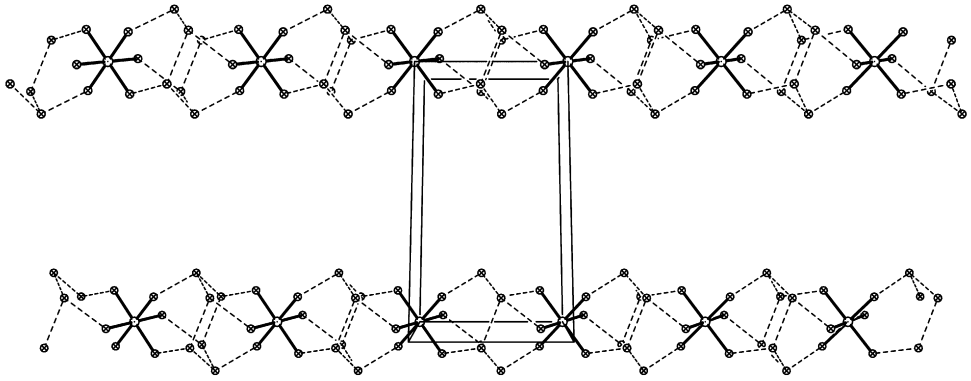

Fig. 3. View of the metal-water chains in $(NH_4)_2[Mn(H_2O)_6][Ti(H_2cit)_3]_2 \cdot 6H_2O$ (**1**) at 30% probability level.

distances [1.873(2), 1.855(1), 1.866(2), 1.867(3), 1.868(2), 1.868(2), and 1.866(2) Å for **1**–**7**] are similar to those found in the previously reported titanium citrate and lactate complexes $(NH_4)_2[Ti(lact)_3]$ [1.848(5) Å] [19] ($H_2$lact = lactic acid). But they are much shorter than those found in peroxo hydroxycarboxylato titanium complexes like $(NH_4)_8[Ti(O_2)(cit)]_4 \cdot 8H_2O$ [2.085(1) Å] and $Ba_2(NH_4)_2[Ti_4(O_2)_4(Hcit)_2(cit)_2] \cdot 10H_2O$ [2.027(3) Å] [20], $(NH_4)_4[Ti(O_2)(cit)]_2 \cdot 2H_2O$ [2.054(2) Å] [21], and $(NH_4)_6[TiO_2(O_2)_4(glyc)_4(Hglyc)_2] \cdot 4H_2O$ [2.029(2) Å] ($H_2$glyc = glycolic acid) [22]. The average Ti–$O_{\alpha\text{-carboxy}}$ distances [2.056(2), 2.035(1), 2.052(2), 2.052(3), 2.047(2), 2.047(2), and 2.049(2) Å for **1**–**7**] are in normal range. The distances are similar to those of the reported titanium(IV)-hydroxycarboxylate complexes. Similar angles are observed in the reported titanium citrate and a number of other $Ti^{IV}O_6$-core containing complexes, exhibiting octahedral geometry around the titanium(IV) ions.

### 3.3. Solution NMR spectra of complex 6

Owing to the paramagnetic effect of the divalent transition metal ions (Mn, Fe, Co, Ni and Cu), only the NMR data of complex **6** were shown in Fig. 4. The solution $^{13}C$ NMR spectrum of **6** in $D_2O$ revealed the presence of the peaks for the free citrate ligand, which demonstrated that complex **6** existed some dissociation in $H_2O$. Large down field shifts of some $^{13}C$ resonances via coordination are observed for complex **6**. This is compared with the corresponding NMR data in $KH_3$cit at a similar pH 3.4 [$KH_3$cit, $^{13}C$ NMR $\delta_C$ ($D_2O$; ppm), 180.0 $(CO_2)_{\alpha\text{-carboxy}}$, 176.3 $(CO_2)_{\beta\text{-carboxy}}$, 76.1 $(C–O)_{\alpha\text{-hydroxy}}$, 46.0 $(CH_2)_{methylene}$]. The large shifts of α-alkoxy carbon ($\Delta\delta \sim 14.6$ ppm) and α-carboxy carbon ($\Delta\delta \sim 8.4$ ppm) indicate the α-alcohol OH and α-carboxylic acid COOH in citric acid are fully deprotonated, and coordinate to the titanium atom simultaneously. This is in agreement with the conclusion derived from the X-ray crystal structure. The $^1H$ NMR spectrum of complex **6** shows two groups of sharp AB quartet for methylene protons, which also corroborates the dissociation of the titanium(IV) citrate complex in aqueous solution.

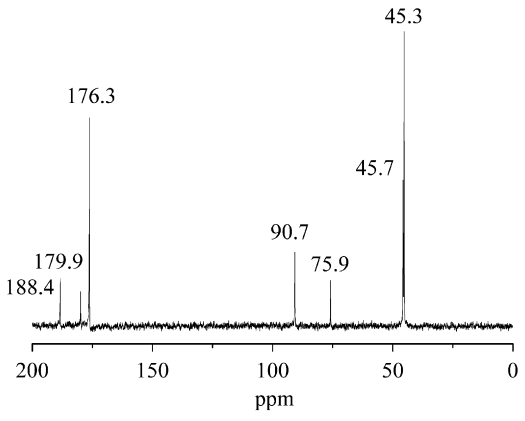


Fig. 4. $^{13}$CNMR spectra of $(NH_4)_2[Zn(H_2O)_6][Ti(H_2cit)_3]_2 \cdot 6H_2O$ (**6**).

### 3.4. Thermal analyses

In order to investigate the crystalline behavior and find out the optimum calcining temperature of the citrate complexes, thermogravimetric (TG) and DSC were conducted and illustrated in Fig. 5 and Figs. S4–S9. Because of the similar thermal decomposition behavior of all of the seven complexes, herein, only the TG and DSC curves of complex **7** are discussed. As shown in Fig. 5, the TG curve shows three main regions of weight loss. The first weight loss of 10.5% appears approximately in the temperature of 25–130 °C. The endothermic peak at 115 °C is probably due to the departure of the six crystalline water molecules and two ammonium cations (theoretical weight loss 9.6%) from complex **7**. The subsequent thermal decomposition of the dehydrated residue in the range of 130–600 °C is complicated. The DSC curve shows three main thermal events, an endothermic peak at 195 °C, an exotherm at 375 °C, and an intense exotherm at 540 °C. The basic thermal decomposition scheme is similar to as those described of $Ba[Ti(H_2cit)_3] \cdot 4H_2O$ [23]. That is, the endotherm at 195 °C being related to the dehydration of the citrate ligand, the exotherms at 375 and 540 °C to the combustion of the organic components. The whole process of the weight loss from 25 to 620 °C is 13.9% for complex **7**, which corresponds to the theoretical weight loss in the case of complete conversion of **7** to $MgTi_2O_5$ with 13.3% weight loss.

### 3.5. X-ray diffraction of the oxides

The X-ray diffraction studies of the calcined heterobimetallic titanium citrate complexes show the products resulting from the thermal treatment. Most of the calcined oxides are mixed oxides as shown in Table S2. Only pure ternary oxides $MgTi_2O_5$ is obtained from the heterometallic complex **7** [24] at 600 and 900 °C as shown in Fig. 6. This is consistent with the orthorhombic system with *Bbmm* space group, in which the cell parameters are 9.712, 10.019 and 3.736 Å, respectively. The size of the resulted particles of $MgTi_2O_5$ phase are between 20 and 30 nm from the calcined product at 600 °C. Its TEM is shown in Fig. 7. The calcined products between 700 and 800 °C are the mixture of $MgTiO_3$, $MgTi_2O_5$ and rutile phases, which further converted to $MgTi_2O_5$ at high temperature. This indicates that further systematic studies are needed by the use of Pechini process, which could be used to obtain the single-phase compounds of the other Ti-based oxides.

## 4. Conclusions

Heterobimetallic titanium citrate complexes have been isolated and characterized for divalent metal ions like $Mn^{2+}$, $Fe^{2+}$, $Co^{2+}$, $Ni^{2+}$, $Cu^{2+}$, $Zn^{2+}$, and $Mg^{2+}$ in an

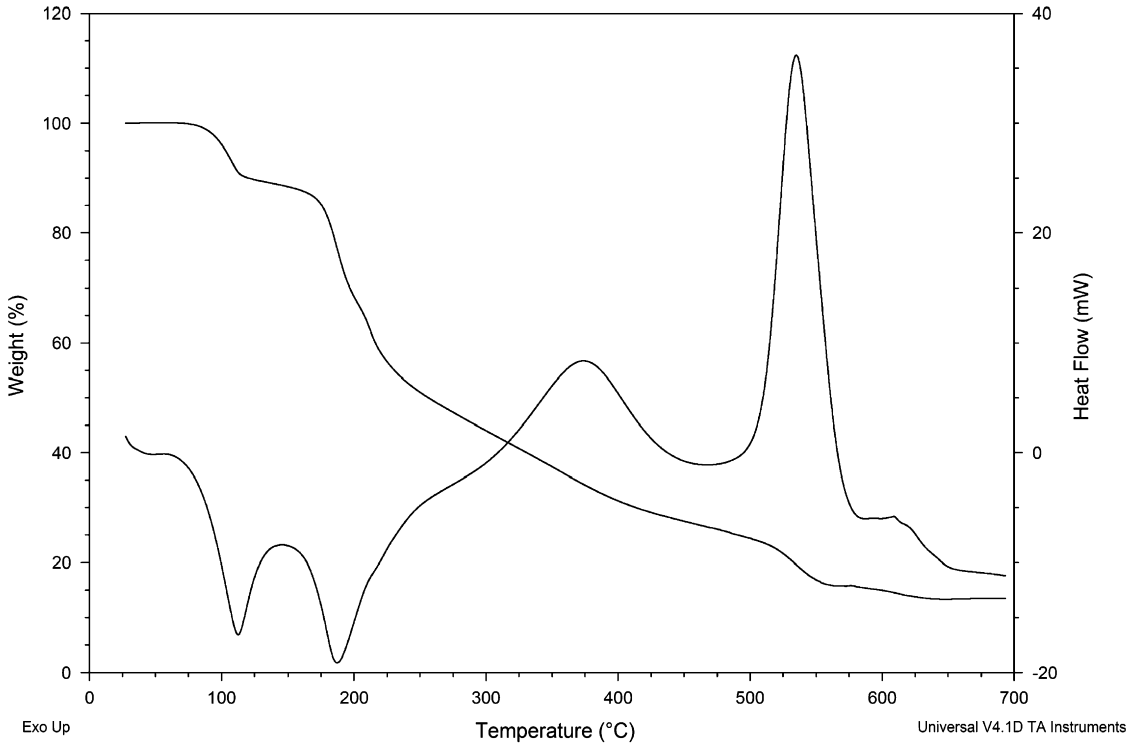


Fig. 5. TG and DTA curves for $(NH_4)_2[Mg(H_2O)_6][Ti(H_2cit)_3]_2 \cdot 6H_2O$ (**7**) (Sample weight: 10.01 mg, rate of heating: 10 °C/min, air).

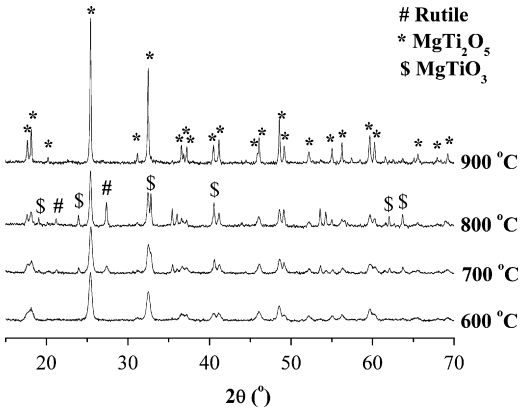


Fig. 6. XRD patterns of $(NH_4)_2[Mg(H_2O)_6][Ti(H_2cit)_3]_2 \cdot 6H_2O$ (**7**) heated at various temperature, with holding 2 h in static air.

acid solution. Citrate ligand displays much better coordination ability toward titanium(IV) cation than the related divalent metal ions at low pH value. The crystal structural study showed a dodecameric water cluster built around a cyclic chair hexameric core was existed in the solid state, which is important for the construction of this series of divalent metal–titanium citrate complexes. The isomorphous suprastructure is constructed with different metal ions between the radius of $Mn^{2+}$ 0.83 and $Ni^{2+}$ 0.69 Å [18]. Thermal decomposition of complex **7** in air at 600 °C provides pure oxide ($MgTi_2O_5$). The use of heterometallic complex as a single source precursor presents the stoichiometry of the final oxides is not merely determined by the composition of the precursors.

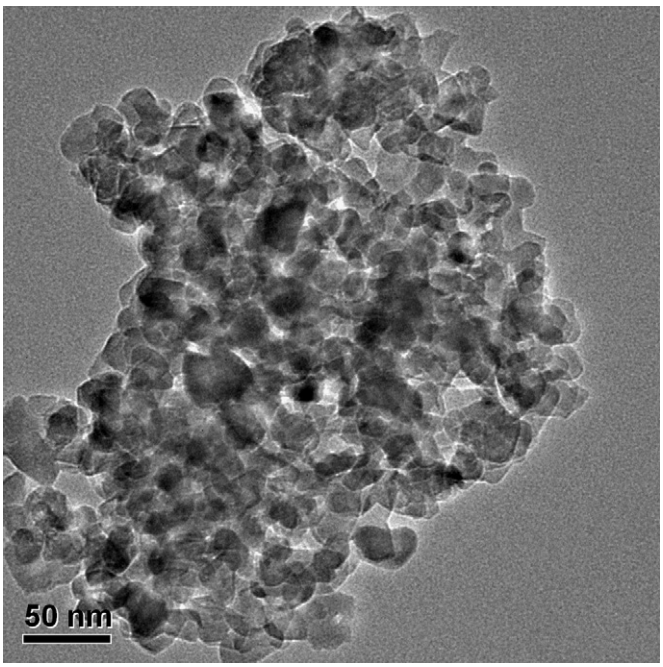


Fig. 7. TEM image of $MgTi_2O_5$ from the thermal decomposition of $(NH_4)_2[Mg(H_2O)_6][Ti(H_2cit)_3]_2 \cdot 6H_2O$ (**7**) at 600 °C.

## Acknowledgments

This work is supported by the National Science Foundation of China (20571061), the Ministry of Science and Technology (2005CB221408) and the Key Scientific Project of Fujian Province, China (2005HZ01-3).

## Appendix A. Supporting information available

Crystallographic data for the structures reported in this paper have been deposited with the Cambridge Crystallographic Data Centre as Supplementary Publication no. CCDC 629904–629909. Copies of the data can be obtained free of charge via http://www.ccdc.cam.ac.uk/conts/retrieving.html, or from the Cambridge Crystallographic Data Centre, 12 Union Road, Cambridge CB2 1EZ, UK; fax: +44 1223 336 033; or e-mail: deposit@ccdc.cam.ac.uk. X-ray crystallographic files in CIF format. IR spectra, thermogravimetric analysis and XRD data are available via the Internet.

## Appendix B. Supplementary materials

Supplementary data associated with this article can be found in the online version at doi:10.1016/j.jssc.2007.08.033.

## References


[1] (a) M.P. Pechini, US Patent No. 3231328, 1966;
(b) M.P. Pechini, US Patent No. 3330697, 1967.
[2] C.D. Chandler, C. Roger, M.J. Hampden-Smith, Chem. Rev. 93 (1993) 1205.
[3] (a) X. Bokhimi, J.L. Boldú, E. Muñoz, O. Novaro, Chem. Mater. 11 (1999) 2716;
(b) T.T. Fang, M.S. Wu, J.D. Tsay, J. Am. Ceram. Soc. 85 (2002) 2984;
(c) Y.X. Pan, Q. Su, H.F. Xu, T.H. Chen, W.K. Ge, C.L. Yang, M.M. Wu, J. Solid State Chem. 174 (2003) 69;
(d) F. Zhao, Z.X. Yue, J. Pei, Z.L. Gui, L.T. Li, J. Solid State Chem. 179 (2006) 1720.
[4] (a) Z.H. Zhou, Y.F. Deng, Y.Q. Jiang, H.L. Wan, S.W. Ng, Dalton Trans. (2003) 2636;
(b) Z.H. Zhou, Y.F. Deng, H.L. Wan, Inorg. Chem. 43 (2004) 6266.
[5] (a) SADABS; University of Göttingen: Göttingen, Germany, 1997;
(b) L.J. Farragia, J. Appl. Crystallogr. 32 (1999) 837.
[6] G.M. Sheldrick, Schelxl-97, Program for Refinement of Crystal Structure, University of Göttingen, Germany, 1997.
[7] (a) Z.H. Zhou, Y.F. Deng, H.L. Wan, Cryst. Growth Des. 5 (2005) 1109;
(b) M. Kotsakis, C.P. Raptopoulou, V. Tangoulis, A. Terzis, J. Giapintzakis, T. Jakusch, T. Kiss, A. Salifoglou, Inorg. Chem. 42 (2003) 22.
[8] (a) D. Mastropalo, D.A. Powers, J.A. Potenz, H.J. Schugae, Inorg. Chem. 15 (1976) 1444;
(b) R.C. Bott, D.S. Sagatys, D.E. Lynch, G. Smith, C.H.L. Kennard, T.C.W. Mak, Aust. J. Chem. 44 (1991) 1495.
[9] (a) G.Q. Zhang, G.Q. Yang, J.S. Ma, Cryst. Growth Des. 6 (2006) 375;
(b) A.G. Stanislowski, J. Inorg. Biochem. 18 (1983) 187.
[10] M. Matzapetakis, N. Karligiano, A. Bino, M. Dakanali, C.P. Raptopoulou, V. Tangoulis, A. Terzis, J. Giapintzakis, A. Salifoglou, Inorg. Chem. 39 (2000) 4044.
[11] Z.H. Zhou, Y.J. Lin, H.B. Zhang, G.D. Lin, K.R. Tsai, J. Coord. Chem. 42 (1997) 131.
[12] E.T. Kefalas, P. Panagiotidis, C.P. Raptopoulou, A. Terzis, T. Mavromoustakos, A. Salifoglou, Inorg. Chem. 44 (2005) 2596.
[13] J.M. Collins, R. Uppal, C.D. Incarvito, A.M. Valentine, Inorg. Chem. 44 (2005) 3431.
[14] J. Paradies, J. Crudass, F. MacKay, L.J. Yellowlees, J. Montgomery, S. Parsons, I. Oswald, N. Robertson, P.J. Sadler, J. Inorg. Biochem. 100 (2006) 1260.
[15] S. Nishikiori, T. Iwamoto, J. Chem. Soc. Chem. Commun. (1993) 1555.
[16] S. Neogi, G. Savitha, P.K. Bharadwaj, Inorg. Chem. 43 (2004) 3711.
[17] G.A. Jeffrey, An Introduction to Hydrogen Bonding, Oxford University Press, Oxford, 1997.
[18] R.D. Shannon, Acta Crystallogr. A 32 (1976) 751.
[19] M. Kakihana, K. Tomita, V. Petrykin, M. Tada, S. Sasaki, Y. Nakamura, Inorg. Chem. 43 (2004) 4546.
[20] (a) M. Kakihana, M. Tada, M. Shiro, V. Petrykin, M. Osda, Y. Nakamura, Inorg. Chem. 40 (2001) 891;
(b) Y.F. Deng, Z.H. Zhou, H.L. Wan, K.R. Tsai, Inorg. Chem. Commun. 7 (2004) 169.
[21] M. Dakanali, E.T. Kefalas, C.P. Raptopoulou, A. Terzis, G. Voyiatzis, I. Kyrikou, T. Mavromoustakos, A. Salifoglou, Inorg. Chem. 42 (2003) 4632.
[22] K. Tomita, V. Petrykin, M. Kobayashi, M. Shiro, M. Yoshimura, M. Kakihana, Angew. Chem. Int. Ed. 45 (2006) 2378.
[23] M. Kakihana, M. Arima, Y. Nakamura, M. Yashima, M. Yoshimura, Chem. Mater. 11 (1999) 438.
[24] (a) D. Purohit, S. Saha, Ceram. Int. 25 (1999) 475;
(b) T. Lopez, J. Hernandez, R. Gomez, X. Bokhimi, J.L. Boldu, E. Munoz, O. Novaro, A. Garcia-Ruiz, Langmuir 15 (1999) 5689;
(c) X. Bokhimi, J.L. Boldu, E. Munoz, O. Novaro, T. Lopez, J. Hernandez, R. Gomez, A. Garcia-Ruiz, Chem. Mater. 11 (1999) 2716;
(d) H.X. Yang, R.M. Hazen, J. Solid State Chem. 138 (1998) 238;
(e) I.E. Grey, C. Li, I.C. Madsen, J. Solid State Chem. 113 (1994) 62.